Supporting Information (SI)

Construction of Ultra-Heat-Resistant Explosives via a Strategy of Building Hydrogen-Bond Networks in Heterocyclic Bridges

Chengchuang Li*[ab], Teng Zhu[b], Linan Zhang[b], Jie Tang[b], Yangfan Cheng[a], Quan Wang*[a], Hongwei Yang*[b], Chuan Xiao[c] and Guangbin Cheng*[b]

a. School of Chemical and Blasting Engineering, Anhui University of Science and Technology, Huainan, Anhui, 232001, PR China.

*Corresponding author E-mail: 2025044@aust.edu.cn (C. Li), quanwang@mail.ustc.edu.cn (Q. Wang).

b. School of Chemistry and Chemical Engineering, Nanjing University of Science and Technology, Xiaolingwei 200, Nanjing, Jiangsu, China.

*Corresponding author E-mail: hyang@mail.njust.edu.cn (H. Yang), gcheng@mail.njust.edu.cn (G. Cheng).

c. China Northern Industries Group Co., Ltd. (NORINCO GROUP), Beijing 100089, P. R. China

Table of Contents

1. Experimental sections

General methods

^{1}H and ^{13}C NMR spectra were recorded on 500 MHz (Bruker AVANCE 500) nuclear magnetic resonance spectrometers operating at 500 and 126 MHz, respectively, by using DMSO-d6 as the solvent and locking solvent unless otherwise stated. Chemical shifts in ^{1}H and ^{13}C NMR spectra are reported relative to DMSO. DSC was performed in closed Al containers with a nitrogen flow of 30 mL min^{-1} on an STD-Q600 instrument. Infrared (IR) spectra were recorded on a Perkin-Elmer Spectrum BX FT-IR equipped with an ATR unit at 25 °C. Impact sensitivity and friction sensitivity of samples are measured by using the standard BAM methods.

Synthesis

3,5-dinitro-N2,N6-diphenylpyridine-2,4,6-triamine (**4**):

Compound **3** (10 mmol, 2.51 g) was added slowly to aniline (20 mL) under gentle stirring. The mixture was stirred continuously to ensure complete dispersion. The temperature was gradually raised to 80 °C and maintained under isothermal conditions with constant stirring for 12 h, during which the stirring rate was kept uniform. After completion of the reaction, the mixture was filtered, and the resulting red powdery precipitate of compound **4** was collected (3.1 g, 86.1%). ^{1}H NMR (500 MHz, DMSO-d6): δ = 6.63 (s, 2H), 7.22 (s, 4H), 7.30 (s, 4H), 10.34 (s, 2H), 11.28 (s, 2H) ppm. ^{13}C NMR (126 MHz, DMSO-d6): δ = 118.6, 121.9, 126.0, 126.1, 129.0, 129.7, 137.6 ppm. IR (KBr): ṽ 3322.2, 3248.9, 3202.5, 3140.4, 3089.7, 1579.2, 1560.3, 1523.9, 1518.6, 1463.2, 1378.0, 1352.0, 1330.8, 1306.2, 1251.8, 1201.2, 1188.8, 773.6, 719.3, 678.8, 635.2, 577.2 cm^{-1}. Elemental analysis for $C_{17}H_{14}N_6O_4$ (366.11): calcd C, 55.74; H, 3.85; N, 22.94%. Found: C55.81, H 3.83, N 22.90%.

3,5-dinitro-2,6-bis((2,4,6-trinitrophenyl)amino)pyridin-4-ol (**5**):

KNO_3 (1.0 g, 10 mmol) was added portionwise to ice-cold concentrated H_2SO_4 (5 mL) with gentle stirring until complete dissolution, taking care to avoid local overheating or splashing. Compound **4** (0.36 g, 1 mmol) was then introduced slowly in small portions under continuous gentle stirring to prevent a sharp temperature rise due to exothermic reaction. The resulting mixture was stirred at room temperature for 30 h with a uniform stirring rate to ensure complete nitration. Upon completion, the reaction mixture was poured slowly into ice water (30 mL) under constant stirring, yielding a yellow powdery precipitate immediately during quenching. Finally, filter the quenched mixture to collect the yellow powdery precipitate, which is the target compound **5** with

a mass of 0.23 g and a yield of 36%. ^{1}H NMR (500 MHz, DMSO-d6): δ = 6.13 (s, 1H), 8.97 (s, 4H), 9.67 (s, 2H) ppm. ^{13}C NMR (126 MHz, DMSO-d6): δ = 120.2, 126.6, 128.6, 129.7, 144.0, 161.3 ppm. IR (KBr): ṽ 3143.7, 3102.3, 3041.6, 3006.8, 2961.8, 1705.0, 1700.6, 1687.6, 1671.1, 1618.1, 1578.9, 1565.1, 1512.2, 1452.3, 1437.5, 1424.3, 1349.5, 1321.4, 1318.8, 1315.4, 1310.2, 1289.6, 1158.3, 1133.2, 921.2, 910.1, 844.0, 811.9, 788.0, 653.6, 567.4 cm^{-1}. Elemental analysis for $C_{17}H_7N_{11}O_{17}$ (638.01): calcd C, 32.04; H, 1.11; N, 24.18%. Found: C 32.15, H 1.10, N 24.08%.

N2,N6-bis(2,4-dinitrophenyl)-3,5-dinitropyridine-2,4,6-triamine (**7**):

Under a nitrogen atmosphere (if required), fuming HNO_3 (2 mL) was added dropwise to ice-cold concentrated H_2SO_4 (5 mL) at –30 °C with gentle stirring. Compound **4** (0.36 g, 1 mmol) was then introduced in small portions under continuous stirring to avoid a rapid exothermic temperature rise. The mixture was subsequently warmed to –20 °C and stirred for 5 h. After completion, the reaction mixture was slowly poured into ice water (20 mL) with constant stirring, immediately affording a white powdery precipitate, which was collected by filtration to give compound **7**. (0.23 g, 43.2%). (0.25 g, 84.5%). ^{1}H NMR (500 MHz, DMSO-d6): δ = 6.58 (s, 2H), 7.56 (s, 2H), 7.77 (s, 2H), 9.04 (s, 2H), 10.57 (s, 2H) ppm. ^{13}C NMR (126 MHz, DMSO-d6): δ = 124.6, 124.9, 125.1, 125.6, 132.8, 141.2, 144.1, 144.7, 147.1 ppm. IR (KBr): ṽ 3328.5, 3259.3, 3147.8, 3074.0, 2993.5, 1704.0, 1687.4, 1684.9, 1677.0, 1668.0, 1621.3, 1599.8, 1574.8, 1568.9, 1518.9, 1507.1, 1451.2, 1363.4, 1317.6,1296.7, 1266.4, 1081.3, 931.3, 925.4, 813.4, 744.9, 656.8, 567.4 cm^{-1}. Elemental analysis for $C_{17}H_{10}N_{10}O_{12}$ (546.05): calcd C, 37.37; H, 1.85; N,25.64%. Found: C 37.31, H 1.86, N 25.69%.

3,5-dinitro-N2,N6-bis(2,4,6-trinitrophenyl)pyridine-2,4,6-triamine (**8**):

Fuming HNO_3 (2 mL) was added dropwise to ice-cold concentrated H_2SO_4 (5 mL) at –30 °C with gentle stirring. Compound **4** (0.36 g, 1 mmol) was then introduced in small portions under continuous stirring to suppress the exothermic temperature rise. The mixture was subsequently warmed to 0 °C and stirred for 5 h. Upon completion, the reaction mixture was slowly poured into ice water (20 mL) with constant stirring, immediately affording a white powdery precipitate, which was collected by filtration to give compound **8** (0.56 g, 88.0%). ^{1}H NMR (500 MHz, DMSO-d6): δ = 9.02 (s, 4H), 9.72 (s, 2H), 10.87 (s, 2H) ppm. ^{13}C NMR (126 MHz, DMSO-d6): δ = 120.2, 123.8, 125.6, 128.5, 129.7, 134.6, 144.0 ppm. IR (KBr): ṽ 3327.9, 3253.1, 3147.7, 3074.9, 2995.6, 1714.7, 1687.8, 1687.2, 1677.2, 1670.1, 1622.3, 1599.0, 1585.7, 1560.2, 1517.2, 1517.8, 1445.0, 1363.2, 1317.9,1296.7, 1266.5, 1081.2, 930.1, 928.2, 813.3,

689.3, 656.2, 567.8, 316.0 cm^{-1}. Elemental analysis for $C_{17}H_8N_{12}O_{16}$ (636.02): calcd C, 32.09; H, 1.27; N, 26.42%. Found: C 32.02, H 1.29, N 26.47%.

2. Computational details of HOF

Computations were performed by using the Gaussian09 suite of programs. [1] The elementary geometric optimization and the frequency analysis were performed at the level of the Becke three parameter, Lee-Yan-Parr (B3LYP) functional with the 6-311+G** basis set. [2-4] All of the optimized structures were characterized to be local energy minima on the potential surface without any imaginary frequencies. Atomization energies were calculated by the CBS-4M. [5]

The predictions of heats of formation (HOF) of compounds used the hybrid DFTB3LYP methods with the 6-311+G** basis set through designed isodesmic reactions. The isodesmic reaction processes, that is, the number of each kind of formal bond is conserved, were used with the application of the bond separation reaction (BSR) rules. The molecule was broken down into a set of two heavy-atom molecules containing the same component bonds. The isodesmic reactions used to derive the HOF shown in Scheme S1.

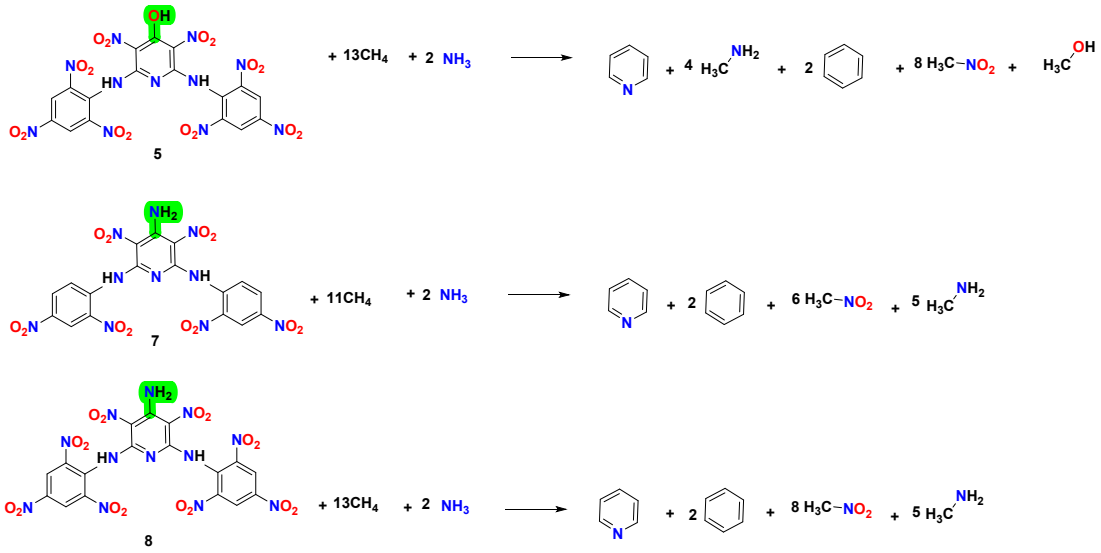

Scheme S1. The isodesmic reactions for calculating heat of formation.

The change of enthalpy for the reactions at 298K can be expressed by Equation (1):

$$\Delta H_{298} = \Sigma\Delta_f H_P - \Sigma\Delta_f H_R \qquad (1)$$

Where $\Sigma\Delta_f H_P$ and $\Sigma\Delta_f H_R$ are the *HOF* of the reactants and products at 298 K, respectively, and ΔH_{298} can be calculated from the following expression in Equation (2):

$$\Delta H_{298} = \Delta E_{298} + \Delta(PV) = \Delta E_0 + \Delta ZPE + \Delta H_T + \Delta nRT \qquad (2)$$

where ΔE_0 is the change in total energy between the products and the reactants at 0 K; ΔZPE is the difference between the zero-point energies (*ZPE*) of the products and the reactants at 0 K; ΔH_T is the thermal correction from 0 to 298 K. The $\Delta(PV)$ value in Equation (2) is the *PV* work term. It equals ΔnRT for the reactions of an ideal gas. For the isodesmic reactions $\Delta n = 0$, so $\Delta(PV) = 0$. On the left side of Equation (2), apart from target compound all the others are called reference compounds. The HOF of reference compounds are available either from experiments or from the high level computing such as CBS-4M.

Table S1 Total energy and heat of formation for the reference compounds

	E_0/a.u.	*ZPE* / kJ·mol^{-1}	ΔH_T / kJ mol^{-1}	$\Delta H_f(g)$ / kJ mol^{-1}
5	-2533.109558	760.57	69.31	282.86
7	-2104.1796001	780.20	60.12	336.71
8	-2513.284720	790.21	66.21	351.22
	-248.346872	222.93	14.09	110.91
	-232.310601	252.53	14.44	82.93
CH_3OH	-115.760107	128.84	11.27	-205.1
CH_3NH_2	-95.893840	160.78	11.64	-22.50
CH_4	-40.533926	112.26	10.04	-74.60
NH_3	-56.499055	86.27	10.05	-45.9
NH_2NO_2	-245.091555	124.93	11.6	-80.8

For the solid phase species, enthalpies of formation $\Delta H_f(s)$ [6] were calculated as follows:

$$\Delta H_{sub} = aA^2 + b\sqrt{v\sigma_{tot}^2} + c$$

$$\Delta_{H_f(s)} = \Delta_{H_f(g)} - \Delta H_{sub}$$

ΔH_{sub} = sublimation enthalpy; $\Delta H_f(g)$ = the heats of formation for gas-phase; $\Delta H_f(s)$ = the heats of formation for solid-phase; A = the molecular surface area; a = 0.000267; b = 1.650087; c = 2.966078.

Table S2. The Heats of Formation for Gas-, Solid-Phase and Heats of Phase Change for Series of compound **5**, **7** and **8**

Compound	ΔH_{sub}/kJ·mol^{-1}	ΔH_f (g)/kJ·mol^{-1}	ΔH_f (s)/kJ·mol^{-1}
5	101.0	282.9	181.9
7	117.4	336.7	219.3
8	112.6	351.2	238.6

3. Crystallographic data

Table S3. Crystallographic data for **5** and **8**

Crystal	**5**·0.5CH_3CN	**8**·2DMF·0.25methanol·0.625H_2O
CCDC number	2552652	2552653
Empirical Formula	$C_{18}H_{8.5}N_{11.5}O_{17}$	$C_{23.25}H_{24.25}N_{14}O_{18.875}$
Formula weight	657.86	801.81
Temperature [K]	193.00	224.00
Crystal system	monoclinic	monoclinic
Space group	$P2_1/c$	C2/c
a/Å	24.4413(17)	53.010(15)
b/Å	15.6786(9)	7.1911(17)
c/Å	12.9303(9)	37.089(9)
α/ °	90	90
β/ °	104.027(5)	94.411(8)
γ/ °	90	90
Cell volume (Å^3)	4807.2(6)	14126(6)
Formula Z	4	2
Density (g cm^{-3})	1.818	1.508
μ (mm^{-1})	1.461	1.163
F (000)	2664	6604.0
Crystal Size (mm^3)	0.10×0.12×0.13	0.12×0.11×0.1
2θ range for data collection (^{o})	6.758 to 136.47	3.336 to 137.418
Index ranges	-29 ≤ h ≤ 29, -18 ≤ k ≤ 8,	-64 ≤ h ≤ 63, -8 ≤ k ≤ 7,

	$-14 \leq l \leq 15$	$-44 \leq l \leq 43$
Reflections collected	31247	40950
Independent reflections	8529 [R_{int} = 0.0981, R_{sigma} = 0.0904]	12924 [R_{int} = 0.0893, R_{sigma} = 0.0686]
Data/restraints/parameters	8529/115/926	12924/463/1156
Goodness-of-fit on F^2	1.018	1.086
Final R indexes [I>=2σ (I)]	R_1 = 0.0675, wR_2 = 0.1605	R_1 = 0.0932, wR_2 = 0.2218
Final R indexes [all data]	R_1 = 0.1148, wR_2 = 0.1963	R_1 = 0.1886, wR_2 = 0.2852

Caution: Explanation of how to improve models for 8·2DMF·0.25methanol·0.625H_2O

"Diffraction data were integrated with corrections for Lorentz and polarization effects using the SAINT program, followed by absorption correction of the integrated data via the SADABS routine. The crystal structure was initially solved by direct methods with SHELXT-2018, and all non-hydrogen atoms were refined anisotropically by full-matrix least-squares minimization within the OLEX2 platform."

Table S4. Hydrogen bonds for **5**

D-H···A	d(D-H)/ Å	d(H···A)/ Å	d(D···A)/ Å	<(DHA)/ º
N4-- H4A..O2	0.8800	2.3500	2.73(2)	107.00
N4-- H4A..O7	0.8800	1.9700	2.606(5)	128.00
N1-- H1A..O3A	0.8800	2.5900	3.36(3)	146.00
N4-- H4A..N6	0.8800	2.6000	2.911(6)	102.00
N8-- H8..O11	0.8800	1.9000	2.564(6)	130.00
N8-- H8..O12	0.8800	2.1900	2.640(6)	111.00
N15-- H15..O22	0.8800	1.8700	2.564(7)	134.00
N19-- H19..O26	0.8800	1.8800	2.576(5)	134.00

Table S5. Torsion angles for **5**

Parameter	Bond angles (Å)	Parameter	Bond angles (Å)
O1-N1-C1-C2	33(3)	C11-N8-C12-C13	130.6(5)
O2-N1-C1-C2	-150(2)	C11-N8-C12-C17	-49.5(6)
O1-N1-C1-C6	-143(2)	C12-N8-C11-C10	172.1(4)
O2-N1-C1-C6	-35(3)	C12-N8-C11-N5	-7.7(6)
O6-N3-C5-C4	145.1(5)	C24-N15-C21-C22	139.9(5)
O6-N3-C5-C4	-32.5(6)	C28-N16-C24-N15	179.2(4)
O6-N3-C5-C4	149.4(5)	C28-N16-C24-C25	-1.9(6)
O6-N3-C5-C4	-33.0(7)	C24-N16-C28-N19	179.6(4)

Table S6. Hydrogen bonds for **8**

D-H···A	d(D-H)/ Å	d(H···A)/ Å	d(D···A)/ Å	<(DHA)/ º
N4--H4..O3	0.8700	1.9300	2.575(7)	129.00
N4--H4..N5	0.8700	2.0600	2.75(3)	136.00
N6--H6A..O9	0.8700	1.8600	2.528(8)	132.00
N6--H6A..N7	0.8700	2.4900	2.825(8)	103.00
N6--H6B..O8	0.8700	1.9100	2.567(9)	131.00
N9--H9..O10	0.8700	1.9300	2.558(8)	128.00
N9--H9..N7	0.8700	2.5900	2.892(7)	102.00
N21--H21..O24	0.8700	1.8700	2.573(9)	130.00

Table S7. Torsion angles for **8**

Parameter	Bond angles (Å)	Parameter	Bond angles (Å)
C2-N4-C7-N8	11.1(8)	C12-N9-C11-N8	-11.9(8)
C2-N4-C7-C8	-170.9(5)	C12-N9-C11-C10	170.0(5)

O1-N1-C1-C2	36.2(9)	C11-N9-C12-C13	-113.2(7)
O2-N1-C1-C2	-136.7(7)	C11-N9-C12-C17	68.0(8)
O1-N1-C1-C6	-144.3(6)	N1-C1-C2-N4	6.7(10)
O2-N1-C1-C6	42.8(9)	N1-C1-C2-C3	-171.3(6)
O3-N2-C5-C6	-12.1(11)	N1-C1-C6-C5	170.0(6)
O3-N2-C5-C4	169.4(7)	C2-C1-C6-C5	-2.7(10)

4. Spectrums of compounds

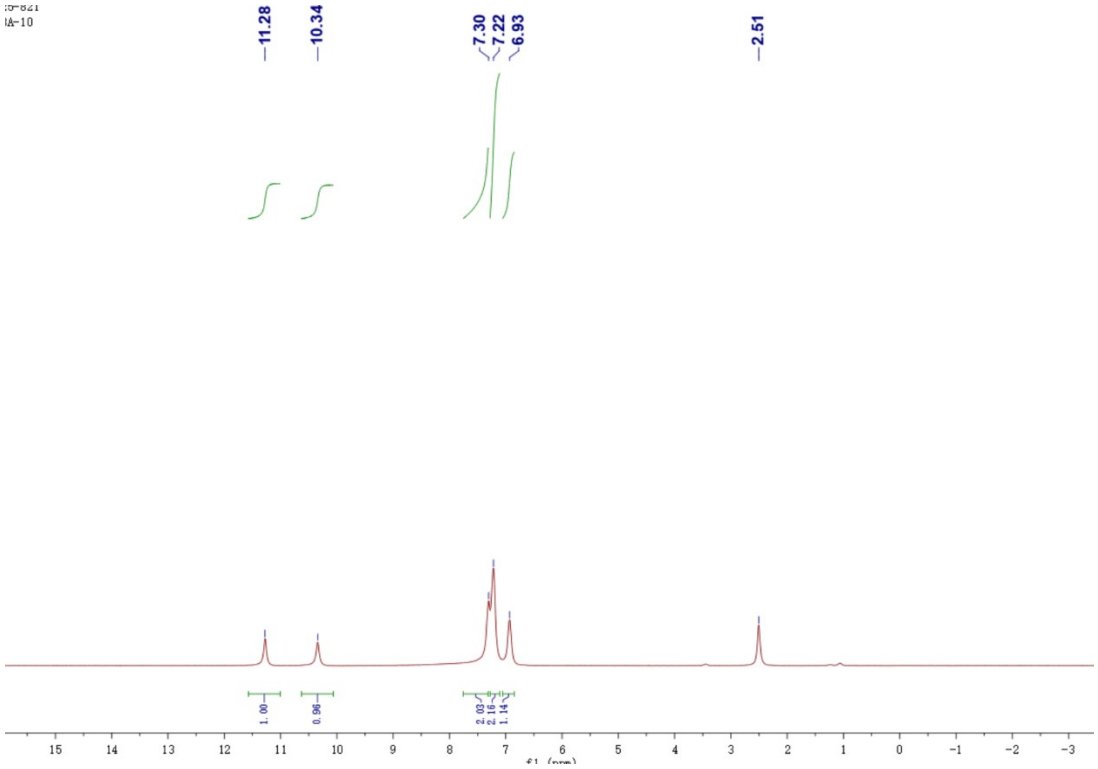

Figure S1. ^{1}H NMR spectra in DMSO-d6 for **4** in DMSO-d6 at 500 MHz

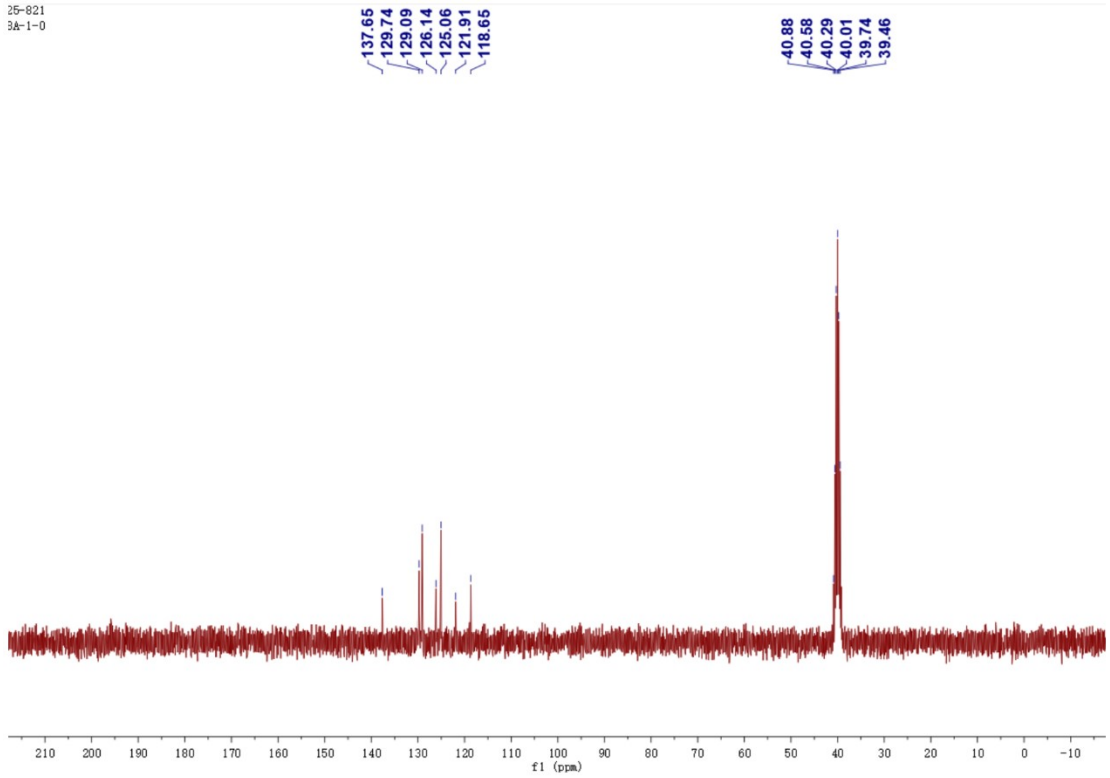

Figure S2. ^{13}C {^{1}H} NMR spectra in DMSO-d6 for **4** in DMSO-d6 at 126 MHz

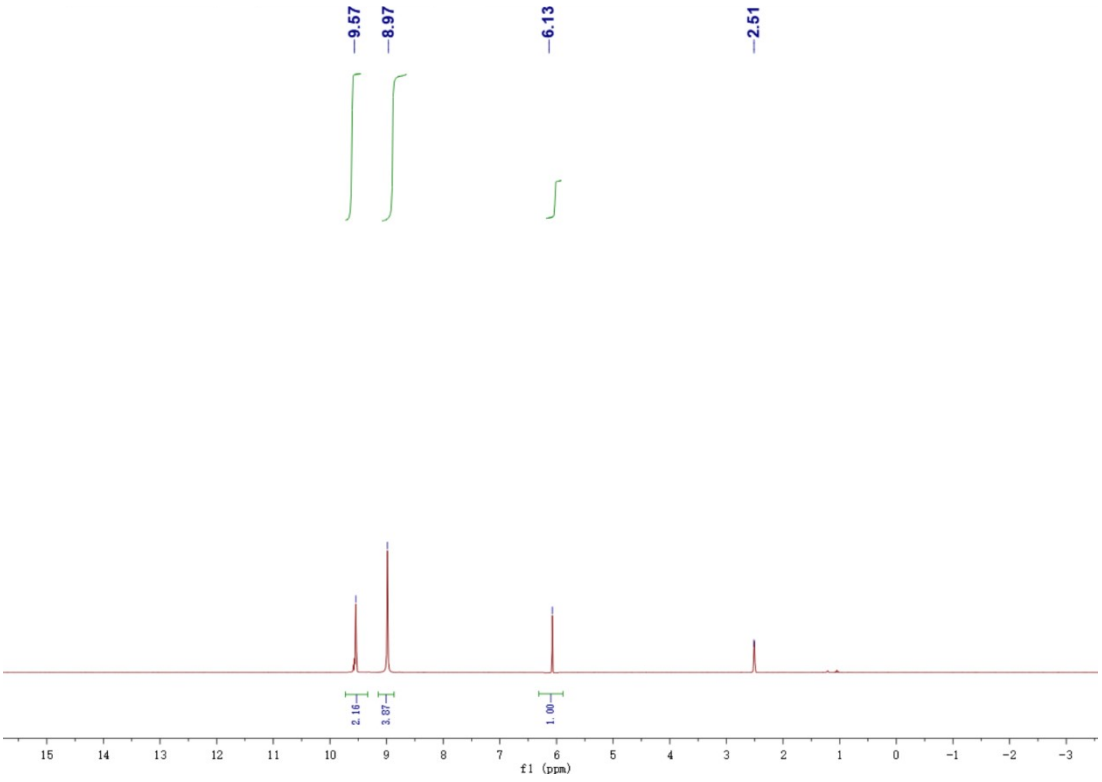

Figure S3. ^{1}H NMR spectra in DMSO-d6 for **5** in DMSO-d6 at 500 MHz

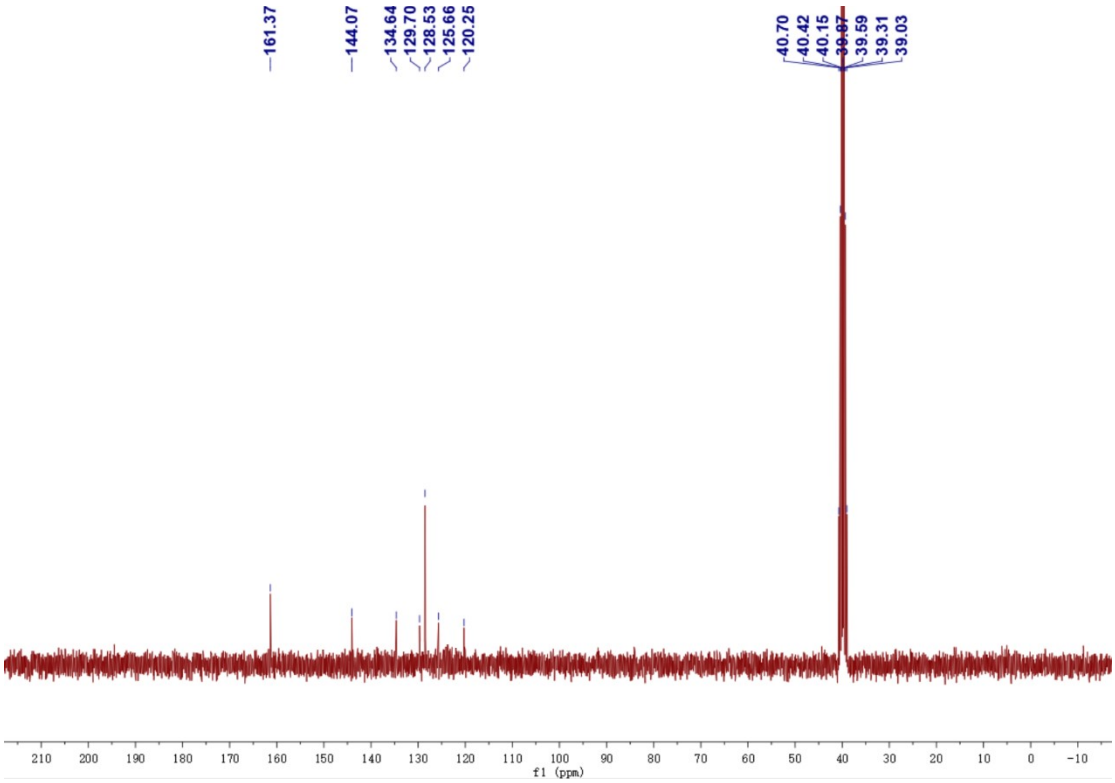

Figure S4. ^{13}C {^{1}H} NMR spectra in DMSO-d6 for **5** in DMSO-d6 at 126 MHz

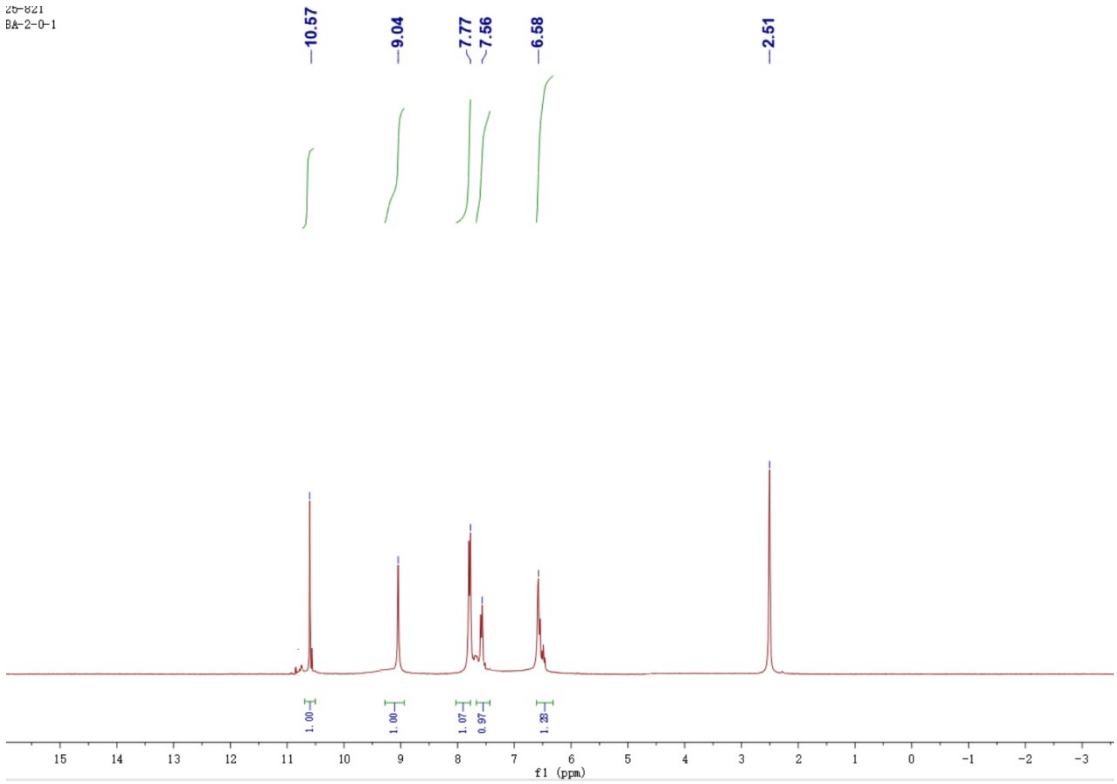

Figure S5. ^{1}H NMR spectra in DMSO-d6 for **7** in DMSO-d6 at 500 MHz

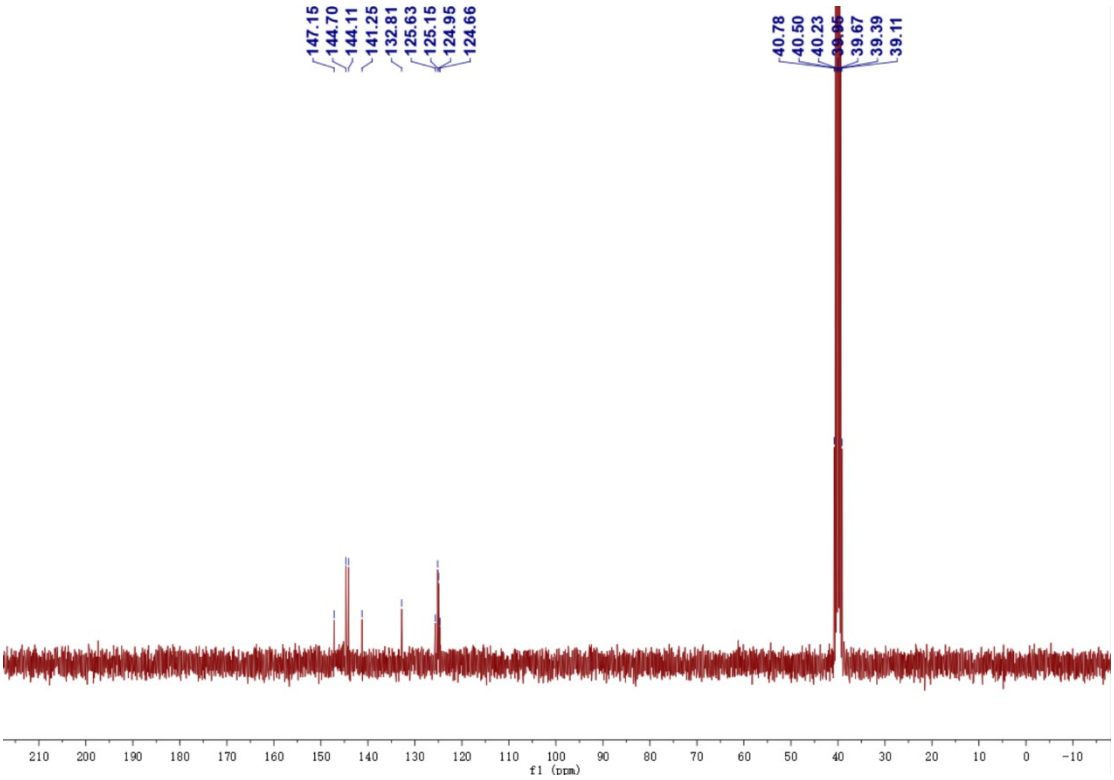

Figure S6. ^{13}C {^{1}H} NMR spectra in DMSO-d6 for **7** in DMSO-d6 at 126 MHz

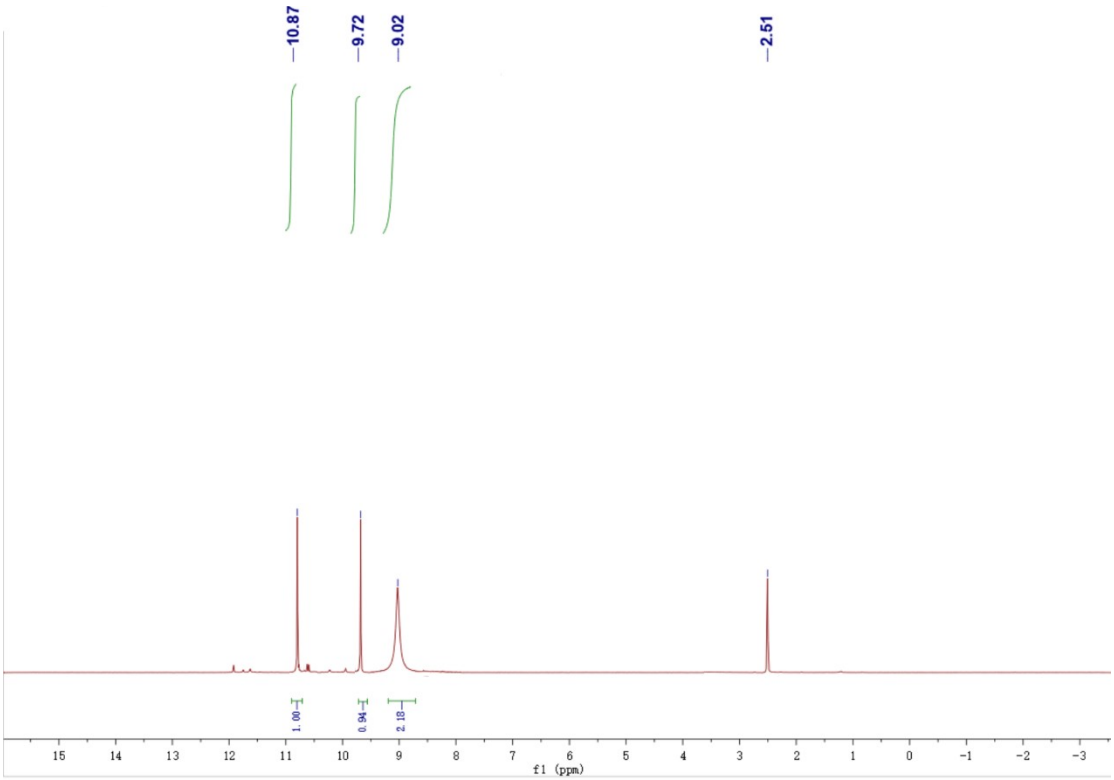

Figure S7. ^{1}H NMR spectra in DMSO-d6 for **8** in DMSO-d6 at 500 MHz

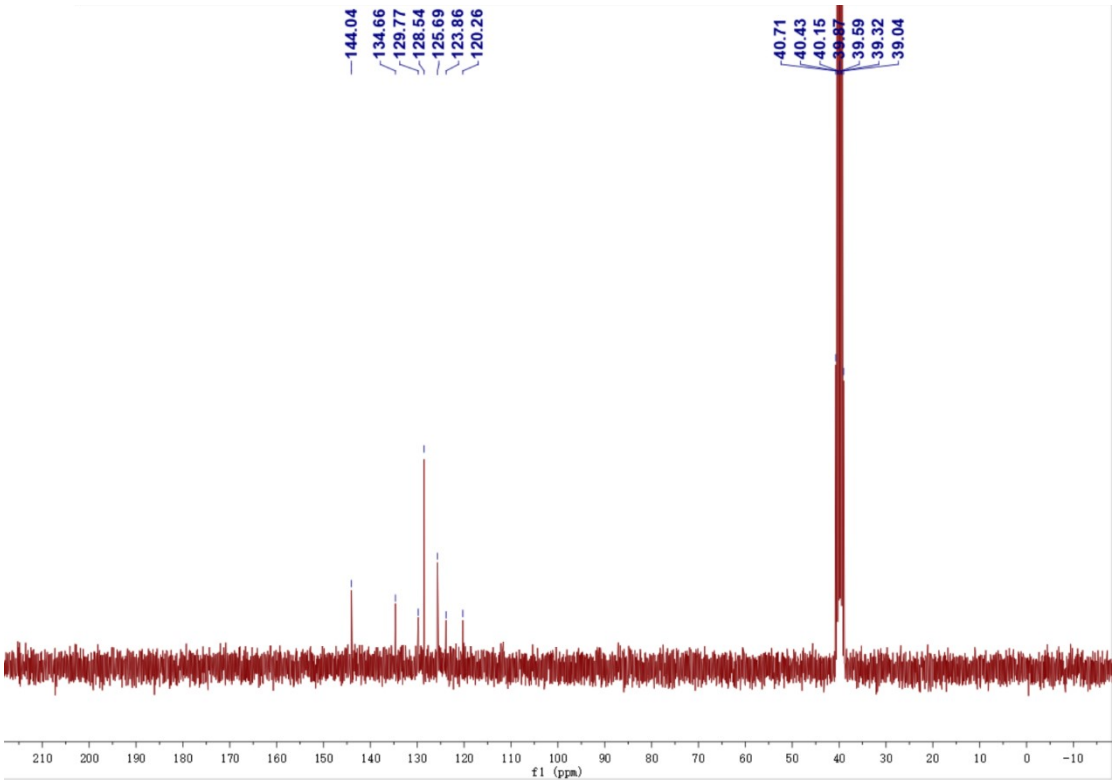

Figure S8. ^{13}C {^{1}H} NMR spectra in DMSO-d6 for **8** in DMSO-d6 at 126 MHz

5. DSC and TG of compounds

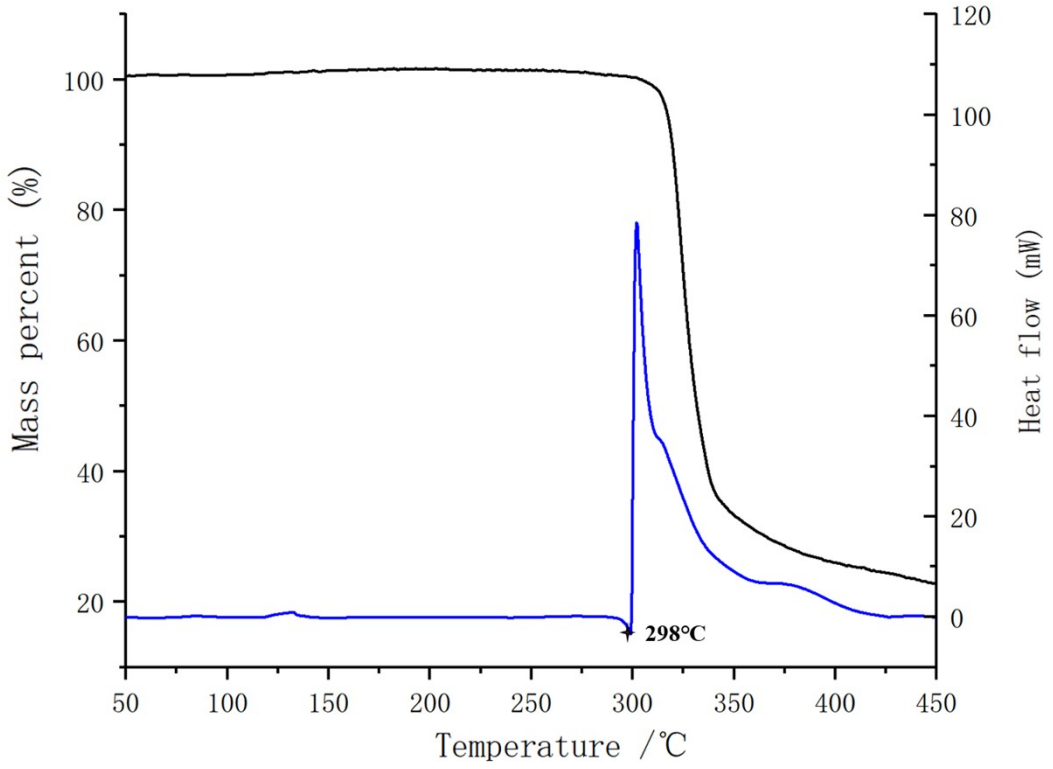

Figure S9 TG and DSC of **5**

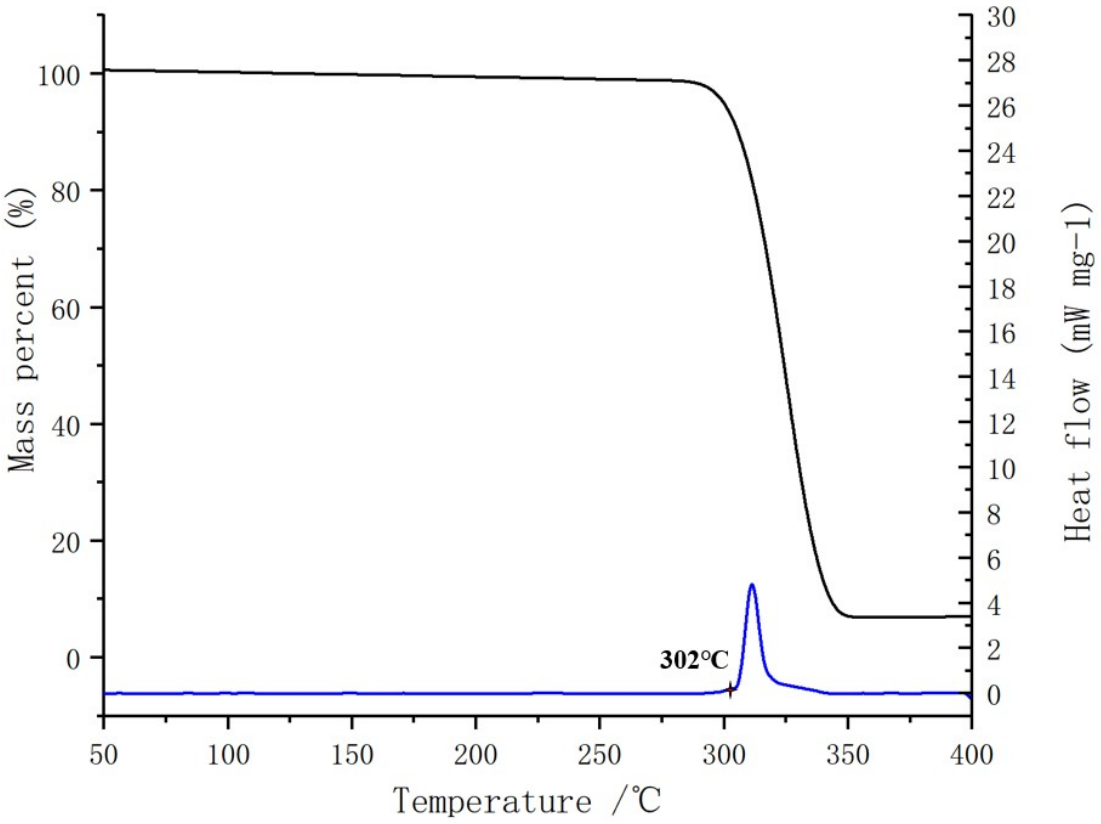

Figure S10 TG and DSC of **7**

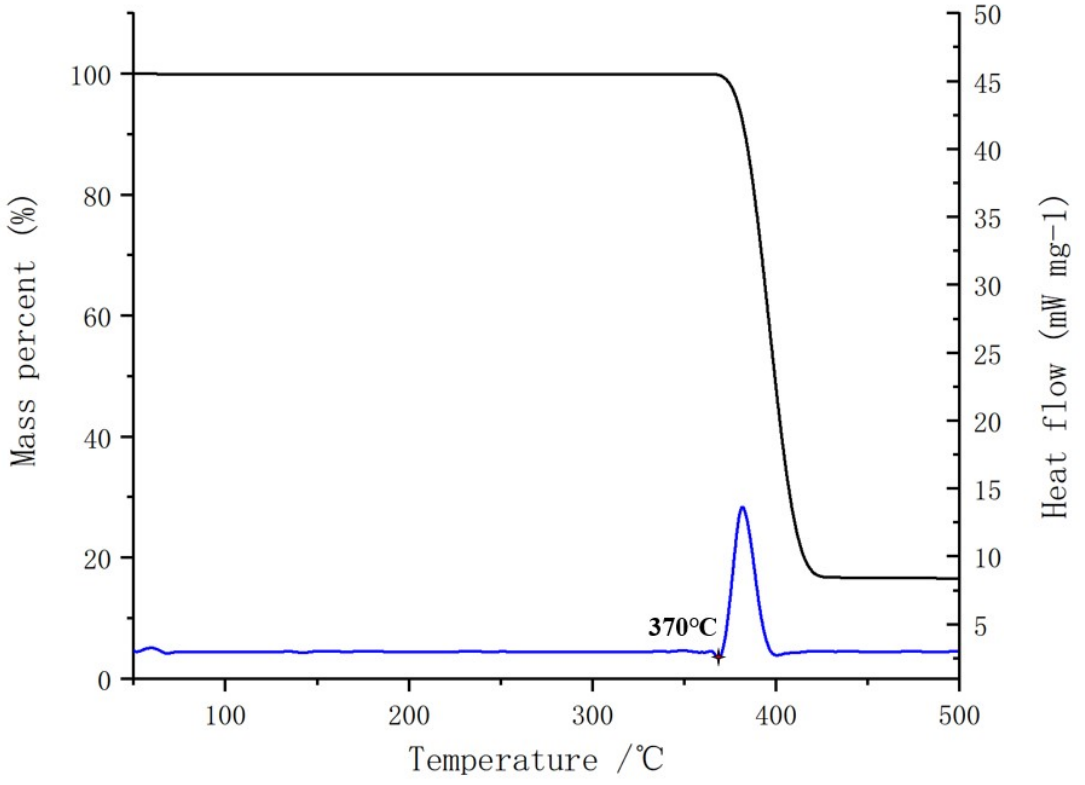

Figure S11 TG and DSC of **8**

6. NCI analysis

Aiming to systematically clarify the origin of the low sensitivity in nitropyridine-bridged tricyclic explosives **5** and **8**, we conducted a comparative study on **5**, PYX, and **8**, which possess the same core skeleton yet feature distinct hydrogen-bond arrangements on the pyridine bridging moieties. In general, the sensitivity of energetic materials is closely correlated with intramolecular and intermolecular hydrogen bonds, as well as π-π stacking interactions. In this work, the non-covalent interaction (NCI) theoretical model was employed to evaluate the weak interaction characteristics of the heterocyclic bridge moieties for the three compounds.[23] Compounds **5** and **8** display slightly larger π–π interaction surfaces compared with PYX, and a large green isosurface between two molecules of **8** is clearly observable. Furthermore, intramolecular hydrogen bonding between adjacent nitro and amino groups in **8** can be readily identified. It is established that extensive π-π interactions and intramolecular hydrogen bonds are beneficial for reducing the mechanical sensitivity of energetic materials, consequently improving their stability and density.

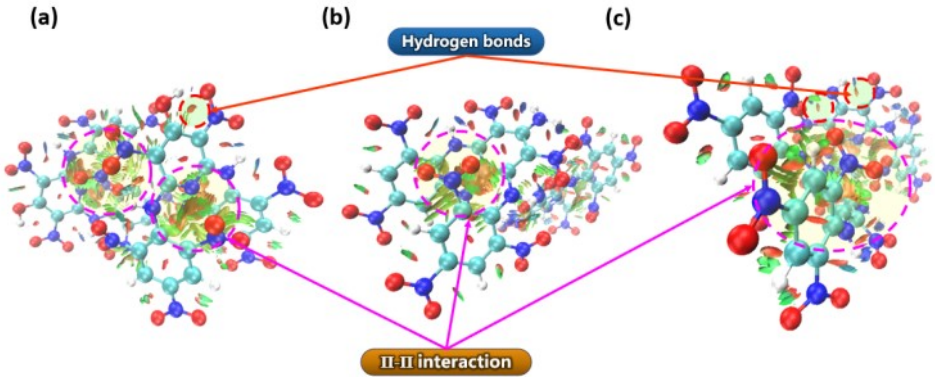

Figure S12 Non covalent interaction (NCI) plots of compounds **5** (a), PYX (b) and **8** (c).

7. References

[1] M. J. Frisch. Gaussian 09, Revision D. 01 (Gaussian Inc., 2009).

[2] A. D. Becke, J. Chem. Phys. **1993**, 98, 5648-5652

[3] P. J. Stephens; F. J. Devlin; C. F. Chabalowski; M. J. Frisch. J. Phys. Chem. **1994**, 98, 11623-11627.

[4] P. C. Hariharan; J. A. Pople, Theor. Chim. Acta. **1973**, 28, 213-222.

[5] J. W. Ochterski; G. A. Petersson; J. A . Montgomery, J. Chem. Phys. **1996**, 104, 2598-2619.

[6] Byrd,E.F.C.;Rice,B.M.J.Phys.Chem.A. **2006**,110 (3),1005−1013.